

Experimental Investigation and Control of a Hybrid (PV-Wind) Energy Power System.

Ghulam Mustafa

Department of Electrical Engineering
Mehran University of Engineering and Technology
Khairpur Mir's, Pakistan
gm_petarian@yahoo.com

Mazhar Hussain Baloch

Department of Electrical Engineering
Mehran University of Engineering and Technology
Khairpur Mir's, Pakistan
mazhar.hussain08ele@gmail.com

Sajid Hussain Qazi

Department of Electrical Engineering
Mehran University of Engineering and Technology
Khairpur Mir's, Pakistan
sajidhussain@muetkhp.edu.pk

Sohaib Tahir

Department of Electrical and Computer Engineering
COMSATS University Islamabad
Sahiwal Campus, Pakistan
sohaibchauhdary@hotmail.com

Noman Khan

Department of Electrical Engineering
Mehran University of Engineering and Technology
Khairpur Mir's, Pakistan
nomankhan@muetkhp.edu.pk

Baqir Ali Mirjat

Department of Electrical Engineering
Mehran University of Engineering and Technology
Khairpur Mir's, Pakistan
baqirali@muetkhp.edu.pk

Abstract—The most essential infrastructure of today's modern civilization is the energy system. A new energy revolution is ongoing worldwide in understanding the affordability, reliability, and sustainability of energy supply. One of the major challenges and opportunities considered in this energy revolution is the integration of the energy system. The varying dynamics of renewable energy production and the environmental conditions between the different energy sources are the major reasons for this challenge. Wind and solar energies are considered the best renewable sources and the foremost substitute sources for power generation. These energies are playing a vital role as alternates of nuclear energy and fossil fuels. Electricity is generated through wind energy conversion systems and photovoltaic (PV) cells. These technologies are clean and environmentally friendlier than non-renewable energies. A hybrid PV-wind generation system is more effective and consistent than a single-source system because the solar system cannot work at night or in cloudy weather while the wind speed is variable. The current study proposes an experimental-based analysis. The hardware used is the Squirrel Cage Induction Generator (SCIG) and solar panels. A boost converter is added for Maximum Power Point Tracking (MPPT) at variable wind speed and available sunlight.

Keywords—WECS; PV cells; SCIG; MPPT

I. INTRODUCTION

Wind and solar energy are the most favorable renewable energy sources due to their low cost of energy production. Many studies have considered only one of these energy sources (solar or wind), which has disadvantages. Wind speed variations disturb the generated power through WECS, whereas

the power produced through PVs is affected by the deviation in solar radiation and varying temperature. Hybrid solar/wind generation is much more effective and consistent, because the solar system cannot work at night or in cloudy weather and wind speed is varying with time and season. Moreover, usually low winds flow on sunny days when solar generation works with higher efficiency [1]. For achieving maximum power, DC/DC converters are used in systems [2-7]. Dual input recommendations are given in [2] in order to get maximum power by using buck/buck boost converters for solar and wind systems. The grid connection of a hybrid system based on solar/fuel and cell/wind was suggested in [3]. Another configuration of multi input booster was proposed for hybrid solar/wind generation systems in [8]. In [1], PMSG machines were utilized for the wind turbine and two DC/DC converters were used for wind and solar energy, whereas in the proposed work, a SCIG machine is used for the wind turbine, to get maximum power and two separate boost converters are used for the wind generator and the PV system. In the proposed model, the characteristic of wind energy conversion system, exhibits maximum power of 3kW and the PV module characteristic exhibits maximum generated power of 44.71W.

II. PROPOSED HYBRID SYSTEM CONFIGURATION

This hybrid system is an assemblage of SCIG based WECS, PV and super capacitor connected MPPT-based boost converters separately at the output of WECS and solar as displayed in Figure 1. The converter is easily controlled by varying the duty cycle with high efficiency and minimum

Corresponding author: Mazhar Hussain Baloch

power variability. The output of both boost converters is connected to a mutual DC bus bar.

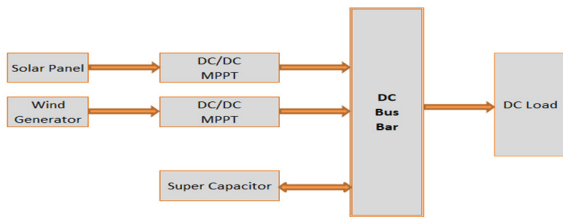


Fig. 1. Diagram of the proposed hybrid system.

A. Maximum Power Point Tracking Algorithm

The algorithm used in this model is P&O (Perturbation and Observation). It is easy to device, low-cost, and simple. The flow chart of P&O MPPT is shown in Figure 2. The scheme constantly perturbs the operative voltage after equating the output power with its earlier value.

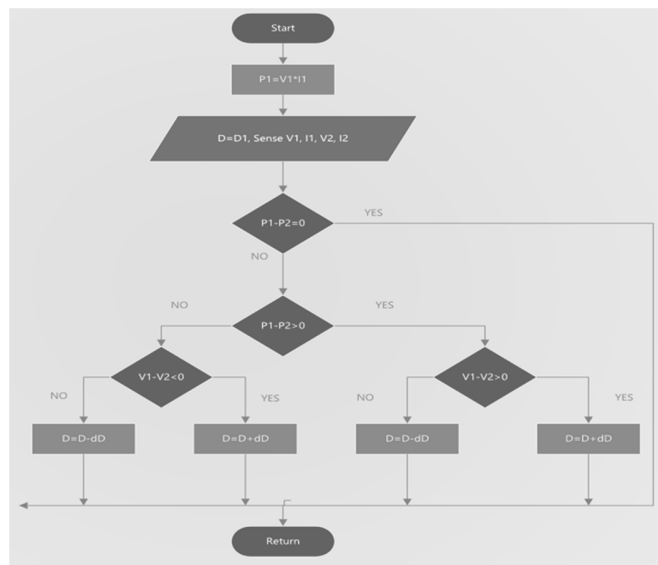


Fig. 2. P&O flow chart.

B. Characteristics of the WECS Generator Model

In the impacted area on the turbine, the power produced is articulated as [9]:

$$P_w = 0.5\rho\pi C_p (\lambda, \beta)^2 V \omega^3 \quad (1)$$

where the co-efficient of power is $C_p=0.3-0.59$, V_ω is the speed of wind, β is the pitch angle for Zone-2 supposing 0° , $\rho=1.25\text{kg/m}^3$, and λ is speed ratio of tip and can be defined by:

$$\lambda = \frac{\omega R}{v} \quad (2)$$

Here, ω is denoted as the rotor speed of the wind generator. Wind power and the turbine power relations are expressed as:

$$P_t = T\omega = Cp(\lambda, \beta)P_w \quad (3)$$

Equation (4) illustrates wind generator's turbine power captured by the wind turbine system. C_p is the performance coefficient, v is free wind speed and ω is the turbine's angular speed.

$$C_p = (0.73)151 \frac{1}{R\omega t} v_\omega - 13 \cdot 635 e \left[\frac{1}{R\omega t} v_\omega - 0.003 \right]^{-1} \quad (4)$$

The turbine power of the wind generator taken by the turbine system is defined by the wind speed given in (4)-(7), whereas the speed of the wind turbine is expressed as in [10, 11]. Equation (5) expresses the power of the wind turbine versus its speed, where P is mechanical power, ρ is air density, and A is the turbine swept area.

$$P_t = 55 \cdot 155 p A \frac{V_\omega}{R\omega t} V_\omega - 0.09 \exp \left[\frac{V_\omega}{R\omega t} - 0.003 \right]^{-1} \quad (5)$$

Figure 3 shows the speed of the wind turbine versus the wind turbine power expressed from (5), where V_w is wind velocity. It should be noted that at different wind speeds, the turbine power changes with respect to the speed of turbine. Figure 3 shows that the turbine power varies at differed wind speeds. The maximum power moves on a 3rd order curve, which shows the maximum power produced by the turbine at each wind speed.

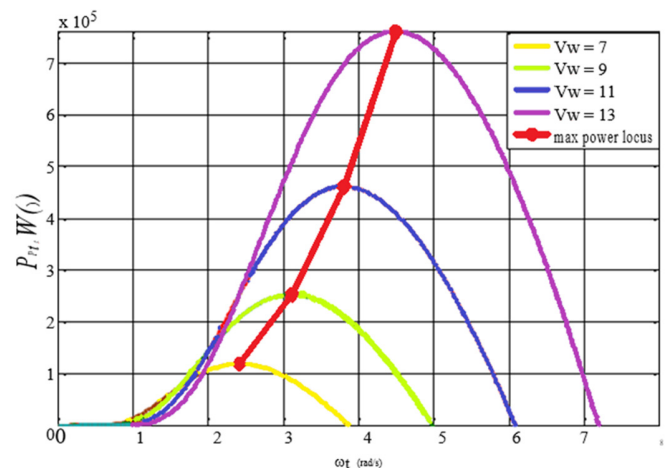


Fig. 3. Turbine power versus turbine speed.

C. Wind Generator System's Controller Model

Through a rectifier wind-generator system, the three-phase AC voltage is inverted to DC voltage (V_{in}) by back electromagnetic force. This review mainly consists on maximum power tracking control performed by the varying duty cycle of the DC-DC boost converter to the DC side. Figure 4 shows the generator control of the DC-DC equivalent circuit. The input voltage adjusted through voltage/current is controlled by the DC-DC boost converter. As a control variable of the duty cycle, the speed of the generator is varied with respect to the turbine in the same proportion.

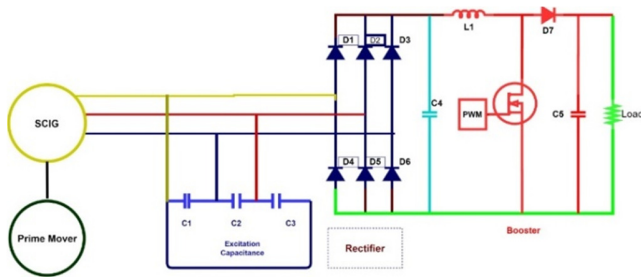


Fig. 4. Circuit diagram with the DC-DC booster converter.

D. PV Cell Modeling

An equivalent circuit of a single PV cell can be shown by applying a source of current, two resistors, and a diode. The model of the PV cell with the single diode is shown in Figure 5, and its description in Table I.

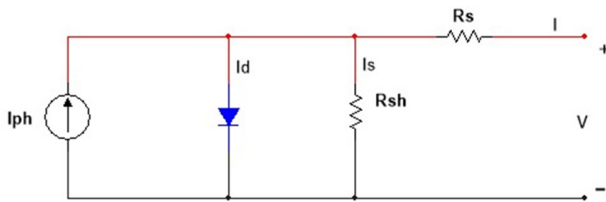


Fig. 5. Equivalent circuit of the PV cell.

The PV cell equation for V-I characteristic is expressed as:

$$I = I_{ph} - I_d - I_{sh} \quad (6)$$

$$= I_{ph} - I_{sc} \left\{ \exp \left[\frac{q}{A_k T_C} (v + IR_s) \right] - 1 \right\} - \frac{v + IR_s}{R_{sh}} \quad (7)$$

where:

$$I_{os} = I_{rs} \left[\frac{T_C}{T_{ref}} \right]^3 \left[\frac{qEg}{B_k} \left(\frac{1}{T_{ref}} - \frac{1}{T_C} \right) \right] \quad (8)$$

$$I_{ph} = [I_{sc} + KI(Tc - 298)] \quad (9)$$

TABLE I. PV MODULE PARAMETERS

Parameter	Variable	Values
Maximum power	P_m	260W
Output tolerance		±3%
Maximum voltage	V_m	30.82V
Maximum current	I_m	8.44A
Open circuit voltage	V_{oc}	36.97V
Short circuit current	I_{sc}	8.94A
Reference solar irradiation	S_{ref}	1000W/m ²
Reference temperature	T_{ref}	25°C
Nominal operating cell temperature	T_{noct}	45±2°C

E. Super-Capacitor

It comprises of two actuated carbon electrodes, which are electrically shielded by an absorbent separator. The current accumulators permit current transferring to the external terminals. The entire system is saturated with electrolyte permitting the ion transportation between both electrodes. Low internal resistance is a property of the super-capacitor. There is contact resistance in the electrode between the current collector and carbon particles, with increase to the non-significant

resistance values given by electrode [12-14]. There are many advantages of super-capacitors for hybrid systems where energy storage devices are needed. The use of these capacitors as secondary power systems allows them to respond quickly during the high load demand. These capacitors have lower time constant than the conventional electrochemical generators (perhaps release charge in a few seconds). Moreover, these capacitors have the ability to deliver bulk power in a very short time. Due to the lack of electrochemical response at the electrodes, the super-capacitors are considered to be used for stability as storage devices [13].

The equivalent model of the super-capacitor is shown in Figure 6. Equation (10) gives the expression of V_{sc} of the voltage of the super-capacitor in relation with the internal resistance R_{sc} and the current I_{sc} of the super-capacitor as:

$$V_{sc} = V1 - R_{sc}I_{sc} = \frac{Q_{sc}}{C_{sc}} - R_{sc}I_{sc} \quad (10)$$

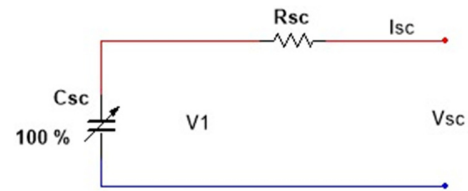


Fig. 6. Equivalent model of the super-capacitor.

For the proposed hybrid system, the super-capacitor is used for storage and stability and is connected to the DC bus. The capacitor bank is shown in Figure 7 and the parameters of the super-capacitor are given in Table II.



Fig. 7. Super capacitor bank.

TABLE II. PARAMETERS OF THE SUPER-CAPACITOR

Characteristic	Value
Rated capacitance (total)	2.640mF
Measured capacitance (total)	2.376mF
Absolute maximum voltage	450V
Rated capacitance of individual cells	0.22mF
Number of cells	12
Temperature	105°C

III. EXPERIMENTAL MODEL AND ANALYSIS

To study the factual and tangible status, the real setup of the wind and solar energy conversion system is required, which is mostly set up to generate simulated controlled wind speed to

operate the WECS and extract solar energy, which requires high cost and big area. A simpler way is software simulation, but it has limitations for real-time investigation. The best way is to follow the wind turbine norms by using a Motor-Generator (MG) setup, where a motor replicates the wind turbine sketch under varying wind speed and a PV panel with artificial generated irradiation represents the solar setup.

TABLE III. EQUIPMENT AND TOOL LIST WITH DESCRIPTION

Equipment name	Description
Prime mover (DC permanent magnet machine)	180Vdc, 2.7A, 0.4KW, 2500rpm. Type:EM-3330-1A, S/N: 201
3 phase squirrel motor (SCIG)	3-phase, 220V, 1.4A, 50/60Hz, 0.3KW, 1420/1670rpm. Type:EM-3330-3C S/N: 201
SolarpPanel	Maximum power 260W
Tachometer	Tachometer 20713A
Rectifier (for 3phase)	PE-5310-5A
Measuring instrument	Company Yalong: YL195 Company Rohde & Schwarz RTH1002
Load (resistor)	3.3kΩ (variable)
Capacitor (excitation cap)	10uf ±5%, 350-400VAC
Super capacitor bank	2.640mF, 450V
Power supply	Power Electronics Universal SupplyMod: AEP-1/EV Capacitor : 470uf 450v*3
Booster	Inductor: 1.8mH 5ADiode: FR205
Digital oscilloscope	GWInstek GDS-2074A, 60Mhz



Fig. 8. Experimental model setup for the hybrid power system.

After ample study, an MG set was taken as a prototype for WECS based entirely on the experimental model. A squirrel cage induction motor machine generated power and a permanent magnet DC machine was chosen to emulate the wind turbine in order to investigate the wind turbine non-linear performance. For the analysis of the output power of SCIG, the motor operated at variable speed. The aim is to experimentally investigate and control the hybrid power system, which is based on WECS and PV through MPPT. The model setup is shown in Figure 8. The WECS was operated with a DC-DC converter connected to the SCIG rectified output. The PV was operated with a DC-DC converter connected to the panel output in order to analyze output factors, i.e. power, voltage, and current. To get the succeeding power values a resistive load was connected as dummy load.

IV. RESULTS AND DISCUSSION

The experimental results of the hybrid wind/PV power system under different scenarios and conditions are discussed below.

Figure 9 shows the bus bar output voltages when both sources are available and ON (hybrid state). Maximum output voltage of 320V is generated by the hybrid system on the bus bar by maintaining the common bus voltage and Figure 10 shows the output current of the hybrid system (0.408A). Figure 11 shows the maximum output power (130.56W) generated by the proposed hybrid system when maintaining common bus power sharing.

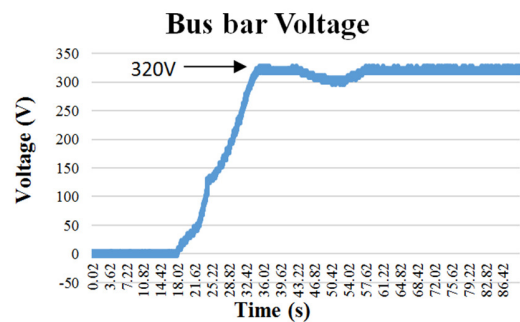


Fig. 9. Bus bar output voltage.

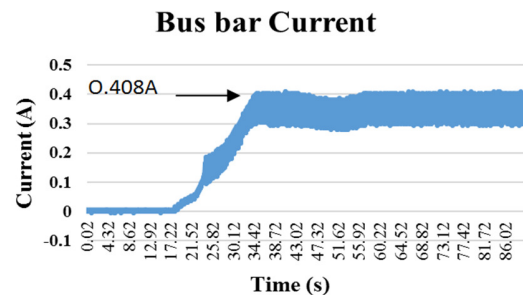


Fig. 10. Hybrid output current.

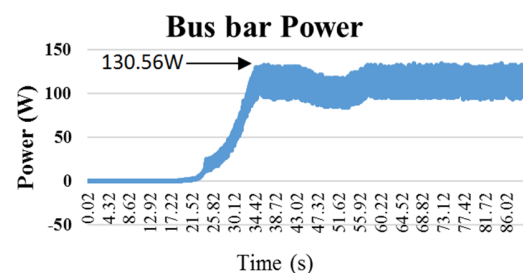


Fig. 11. Hybrid output power.

Figure 12 shows the voltages before and after the boost converter with respect to generator speed (rpm), when WECS us ON and PV is OFF. It is clearly shown from the output results that at 37s a high rectified output voltage of 280V is generated while out of the DC/DC boost converter the output voltage received is 340V. The speed of the generator was 660rpm when these maximum voltages were recorded. So the voltages of WECS before boost converter was augmented by

21% by using the designed boost converter, working on the principle of P&O algorithm.

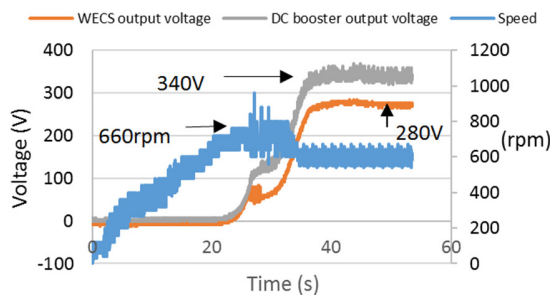


Fig. 12. Output voltages before and after boost w.r.t speed.

Figure 13 shows the voltage before and after the boost converter along with the power after the boost converter (44.71W). It is clearly shown from the output results that at 31s, the maximum generated output voltage of the solar panel is 34V while at out of DC/DC boost converter the output voltage received is 324V. The voltage of the solar source before the boost converter is maximized by using the designed buck-boost converter working on the principles of genetic algorithm. The results are summarized in Table IV.

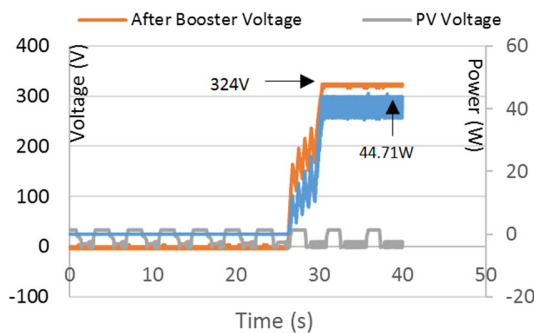


Fig. 13. PV output vs boost converter output.

TABLE IV. RESULT SUMMARY

Hybrid PV-Wind Power System						
S.No.	Wind	Rpm	PV	Irradiation	Voltage	Power
1	ON	660	OFF	N/A	340	100.3
2	OFF	N/A	ON	9.164	324	44.71
3	ON	621	ON	9.164	320	130.56

V. CONCLUSION

The achieved experimental results show the below mentioned conclusions, which can be extracted from this study. At present, standalone wind and PV systems are globally supported on a relatively large-scale but are not able to give consistence energy. The hybrid system based on Wind/PV is a smart scheme for the utilization of the emergent substitute and renewable sources of energy. This study shows a hybrid WECS/PV system connected to a DC bus with MPPT. The analysis and results of the proposed experimental model signified the output power produced by the hybrid scheme

which can supply continuous power with improved consistency in comparison with a single power source system. The results of the system in three different conditions were analyzed.

- When the WECS system was ON and the PV was OFF, the characteristic of wind energy conversion system, exhibited maximum power of 100.3W.
- When the WECS system was OFF and the PV was ON, the PV module characteristic exhibited maximum power of 44.71W.
- When both sources were ON (hybrid state), the maximum power generated by the hybrid system was 130.56W by maintaining the common bus voltages and power-sharing.

The hardware-based experimental model of the hybrid system proved to provide fruitful results under varying environmental conditions. In the proposed model, two boost converters are separately used for PV and wind having MPPT functions. The converters were based on the P&O and Genetic MPPT algorithms, which transferred maximum power to the DC bus from the WECS and the PV cell.

REFERENCES

- [1] S. P. LakshmanRao, C. P. Kurian, B. K. Singh, and V. Athulya Jyothi, "Simulation and Control of DC/DC Converter for MPPT Based Hybrid PV/Wind Power System," *International Journal of Renewable Energy Research*, vol. 4, no. 3, pp. 801–809, Sep. 2014.
- [2] Y. S. Rao, A. J. Laxmi, and M. Kazeminehad, "Modeling and Control of Hybrid Photovoltaic Wind Energy Conversion System," *International Journal of Advances in Engineering & Technology*, vol. 3, no. 2, pp. 192–201, May 2012.
- [3] N. A. Ahmed, A. K. Al-Othman, and M. R. AlRashidi, "Development of an efficient utility interactive combined wind/photovoltaic/fuel cell power system with MPPT and DC bus voltage regulation," *Electric Power Systems Research*, vol. 81, no. 5, pp. 1096–1106, May 2011, <https://doi.org/10.1016/j.epr.2010.12.015>.
- [4] S. Mahesar et al., "Power Management of a Stand-Alone Hybrid (Wind/Solar/Battery) Energy System: An Experimental Investigation," *International Journal of Advanced Computer Science and Applications*, vol. 9, no. 6, Jan. 2018, <https://doi.org/10.14569/IJACSA.2018.090631>.
- [5] M. Muralikrishna and V. Lakshminarayana, "Hybrid (solar and wind) energy systems for rural electrification," *ARPN Journal of Engineering and Applied Sciences*, vol. 3, no. 5, pp. 50–58, Oct. 2008.
- [6] Y. Chen, Y. Liu, S. Hung, and C. Cheng, "Multi-Input Inverter for Grid-Connected Hybrid PV/Wind Power System," *IEEE Transactions on Power Electronics*, vol. 22, no. 3, pp. 1070–1077, May 2007, <https://doi.org/10.1109/TPEL.2007.897117>.
- [7] M. Hussain, M. H. Baloch, A. H. Memon, and N. K. Pathan, "Maximum Power Tracking System Based on Power Electronic Topology for Wind Energy Conversion System Applications," *Engineering, Technology & Applied Science Research*, vol. 8, no. 5, pp. 3392–3397, Oct. 2018, <https://doi.org/10.48084/etasr.2251>.
- [8] B. M. Shagar, S. Vinod, and S. Lakshmi, "Design of DC - DC converter for hybrid wind solar energy system," in *2012 International Conference on Computing, Electronics and Electrical Technologies (ICCEET)*, Kumaracoil, India, Mar. 2012, pp. 429–435, <https://doi.org/10.1109/ICCEET.2012.6203805>.
- [9] M. H. Baloch, J. Wang, and G. S. Kaloi, "Stability and nonlinear controller analysis of wind energy conversion system with random wind speed," *International Journal of Electrical Power & Energy Systems*, vol. 79, pp. 75–83, Jul. 2016, <https://doi.org/10.1016/j.ijepes.2016.01.018>.
- [10] M. Pucci and M. Cirrincione, "Neural MPPT Control of Wind Generators With Induction Machines Without Speed Sensors," *IEEE Transactions on Industrial Electronics*, vol. 58, no. 1, pp. 37–47, Jan. 2011, <https://doi.org/10.1109/TIE.2010.2043043>.

-
- [11] R. Cárdenas, R. Peña, J. Clare, and P. Wheeler, "Analytical and Experimental Evaluation of a WECS Based on a Cage Induction Generator Fed by a Matrix Converter," *IEEE Transactions on Energy Conversion*, vol. 26, no. 1, pp. 204–215, Mar. 2011, <https://doi.org/10.1109/TEC.2010.2083666>.
- [12] A. Kadri, H. Marzougui, A. Aouiti, and F. Bacha, "Energy management and control strategy for a DFIG wind turbine/fuel cell hybrid system with super capacitor storage system," *Energy*, vol. 192, Feb. 2020, Art. no. 116518, <https://doi.org/10.1016/j.energy.2019.116518>.
- [13] O. Erdinc, B. Vural, and M. Uzunoglu, "A wavelet-fuzzy logic based energy management strategy for a fuel cell/battery/ultra-capacitor hybrid vehicular power system," *Journal of Power Sources*, vol. 194, no. 1, pp. 369–380, Oct. 2009, <https://doi.org/10.1016/j.jpowsour.2009.04.072>.
- [14] T. R. Ayodele, A. S. O. Ogunjuyigbe, and B. E. Olateju, "Improving battery lifetime and reducing life cycle cost of a PV/battery system using supercapacitor for remote agricultural farm power application," *Journal of Renewable and Sustainable Energy*, vol. 10, no. 1, Jan. 2018, Art. no. 013503, <https://doi.org/10.1063/1.4999780>.